

Supporting Information

Achieving narrowband emissions with tunable colors for multiple resonance-thermally activated delayed fluorescence materials: Effect of Boron/Nitrogen number and position

Ping Li,^a Yewen Zhang,^a Wenjing Li,^a Cefeng Zhou,^a and Runfeng Chen^{a b*}

^a State Key Laboratory of Organic Electronics and Information Displays & Institute of Advanced Materials (IAM), Nanjing University of Posts & Telecommunications, 9 Wenyuan Road, Nanjing 210023, P. R. China.

^b School of Materials Science and Engineering, Zhejiang Sci-Tech University, Hangzhou 310018, P. R. China

*Corresponding author.

E-mail: iamrfchen@njupt.edu.cn

Contents

Fig. S1 Optimized ground-state structures of the investigated molecules from top and side views.

Fig. S2 Optimized structures at S_1 state of the investigated molecules.

Fig. S3 Diagram of geometry deviations between S_0 and S_1 states for molecular skeleton, peripheral methyl groups and heavy atoms together with the calculated RMSD values.

Fig. S4 Calculated Huang-Rhys (HR) factors versus the normal mode frequencies for the investigated molecules.

Fig. S5 Frontier molecular orbital density distributions, energy levels and HOMO-LUMO gaps of the studied molecules at the optimized S_1 geometry.

Fig. S6 Hole and electron distributions for the investigated molecules.

Fig. S7 Details of the color-filled TDM maps for BN1.

Table S1 Simulated the maximum absorption wavelength (λ_{abs} , nm) of the experimental molecules with different DFT functionals.

Table S2 Simulated the maximum emission wavelengths (λ_{emi} , nm) of the experimental molecules with different DFT functionals.

Table S3 Calculated the maximum absorption and emission energies and wavelengths with B3LYP functional and different basis sets for the investigated experimental molecules.

Table S4 Calculated bond lengths of the studied molecules at S_0 and S_1 states.

Table S5 Calculated the low-lying energies (E_{S1}), the maximum absorption wavelengths (λ_{abs}), oscillator strengths (f), and transition compositions related to $S_0 \rightarrow S_1$ process for the investigated molecules in toluene.

Table S6 Calculated oscillator strength and the square of the transition dipole moment for the investigated molecules relevant to absorption and emission processes.

Table S7 Simulated FWHM at the maximum emission wavelength of the studied molecules.

Computational Methodology

Huang-Rhys (HR) Factor

$$S = \sum S_i = \sum \frac{1}{2} \Delta Q_i^2$$

ΔQ_i refers to the dimensionless displacement of the equilibrium position of the ground state and excited state under the i^{th} vibration mode, and S_i refers to the Huang-Rhys factor of the i^{th} vibration mode.

Reorganization Energy

$$\lambda = \sum \lambda_i = \sum \hbar \omega_i S_i$$

$$\lambda_i = \frac{k_i}{2} \Delta Q_i^2, \quad S_i = \frac{\lambda_i}{\hbar \omega_i}$$

Here, k_i and ω_i are the corresponding force constants and vibrational frequencies, which can be calculated and analyzed from the normal-mode analysis method using the DUSHIN code.

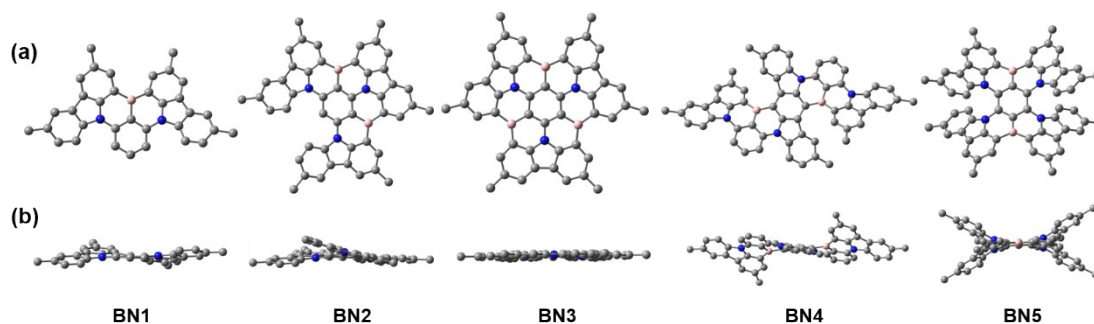


Fig. S1 Optimized ground-state structures of the investigated molecules from top (a) and side (b) views.

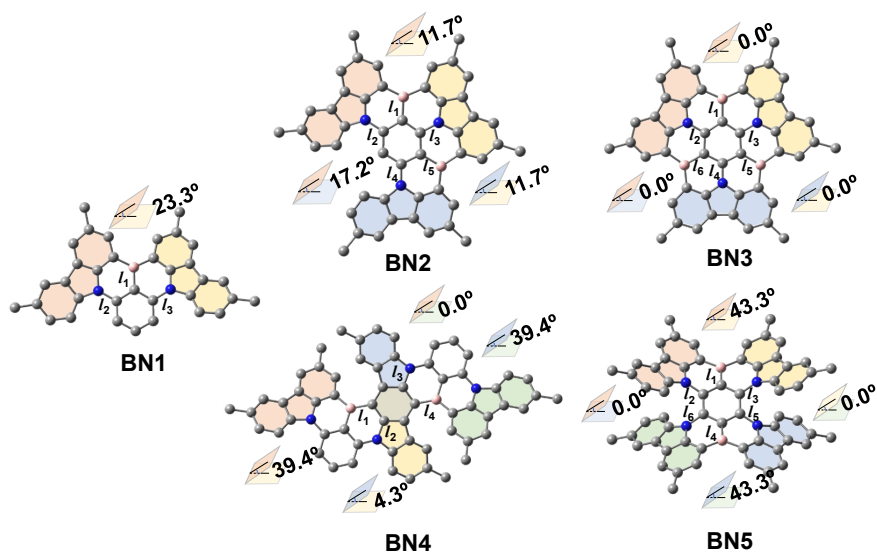


Fig. S2 Optimized structures at S_1 state of the investigated molecules together with the calculated dihedral angles.

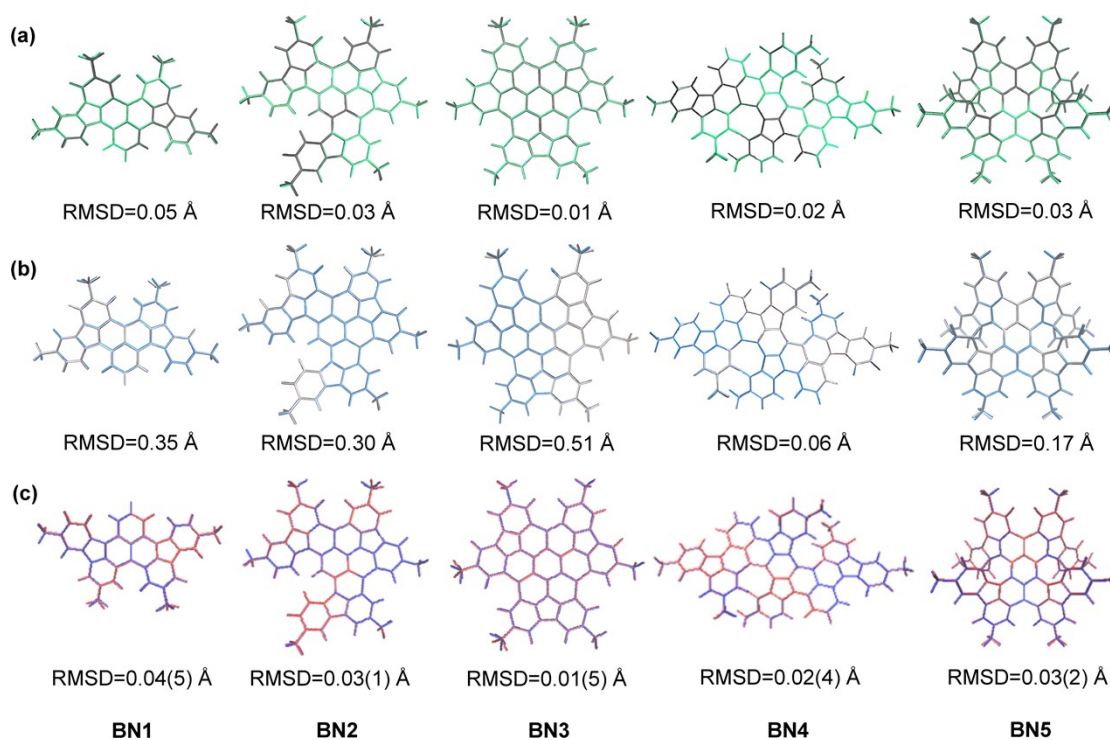


Fig. S3 Diagram of geometry deviations between S_0 and S_1 states for (a) molecular skeleton (the structures at S_0 and S_1 states are depicted in green and red, respectively), (b) peripheral methyl groups (the structures at S_0 and S_1 states are depicted in grey and blue, respectively), and (c) heavy atoms (the structures at S_0 and S_1 states are depicted

in deep-blue and red, respectively) together with the calculated RMSD values.

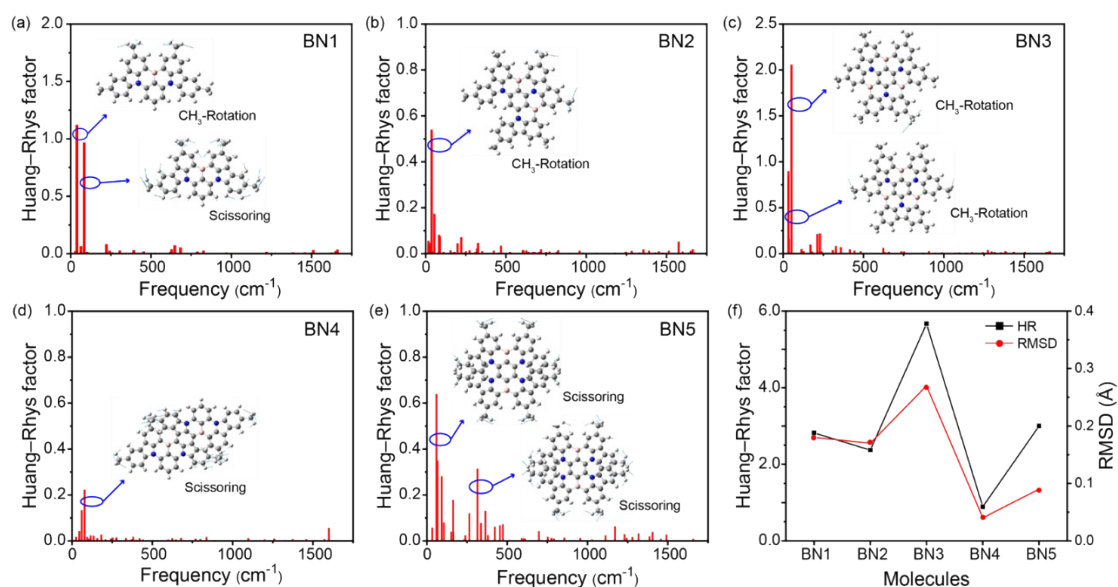


Fig. S4 Calculated Huang-Rhys (HR) factors versus the normal mode frequencies for the investigated molecules of (a) BN1, (b) BN2, (c) BN3, (d) BN4, and (e) BN5 (Vibration modes with large contributions to the HR factors are shown as insets). (f) Changing trend of HR factors and RMSD values.

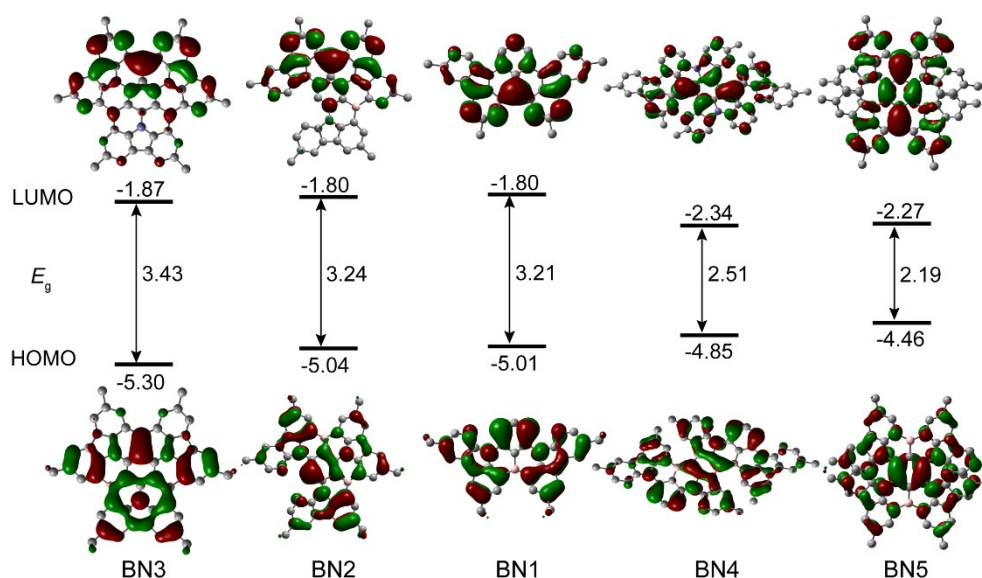


Fig. S5 Frontier molecular orbital density distributions, energy levels and HOMO-LUMO gaps of the studied molecules at the optimized S_1 geometry.

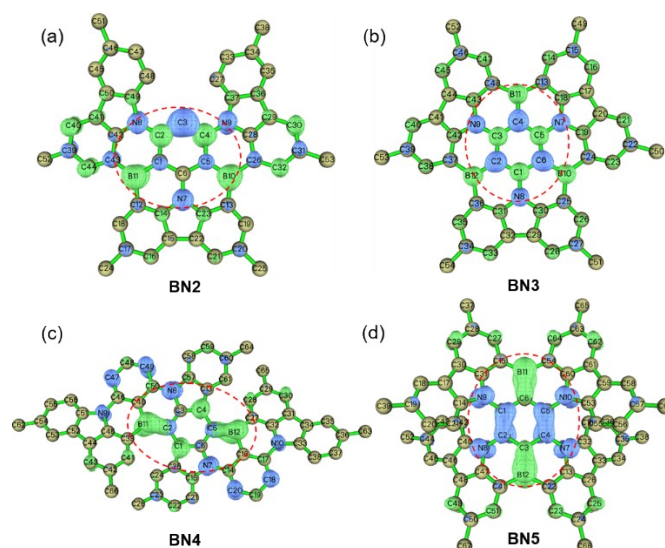


Fig. S6 Hole and electron distributions for the investigated molecules of (a) BN2, (b) BN3, (c) BN4, and (d) BN5.

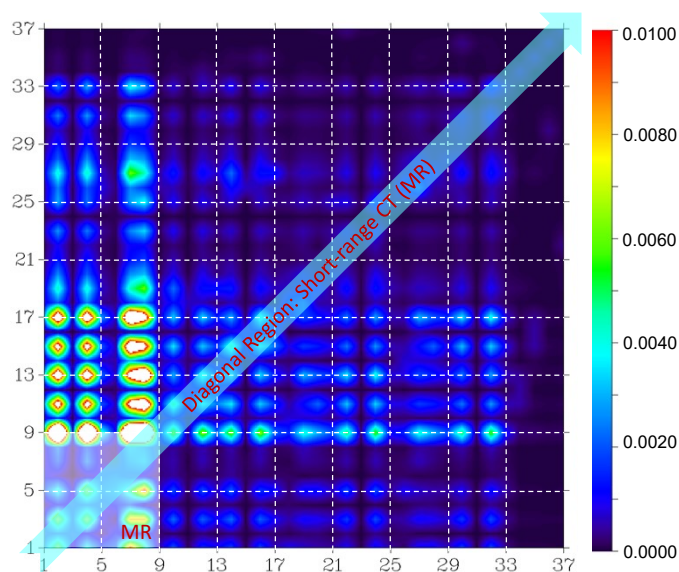


Fig. S7 Details of the color-filled TDM maps for BN1.

Table S1 Simulated the maximum absorption wavelengths (λ_{abs} , nm) of the experimental molecules with different DFT functionals.

Compd.	λ_{abs} (nm)
--------	-----------------------------

	MPW1KCI	B3LYP	PBE0	CAM-	ω B97XD	Exp.
	S (15% HF _{exc})	(20% HF _{exc})	(25% HF _{exc})	B3LYP	(100% HF _{exc})	
	a					
BN1	464	443	429	378	371	468
BN2	455	435	421	373	367	453
BN4	617	582	560	470	458	597
BN5	674	634	613	516	504	629 ^b /651 ^c

^a (19% HF_{exc} at short-range and 65% HF_{exc} at long-range)

^b BN5 without alkyl unit; ^c BN5 with tert-butyl alkyl units

Table S2 Simulated the maximum emission wavelengths (λ_{emi} , nm) of the experimental molecules with different DFT functionals.

Compd.	λ_{emi} (nm)					Exp.
	MPW1KCIS	B3LYP	PBE0	CAM-	ω B97XD	
	(15% HF _{exc})	(20% HF _{exc})	(25% HF _{exc})	B3LYP	(100% HF _{exc})	
	a					
BN1	488	465	448	390	382	489
BN2	479	453	435	379	372	466
BN4	645	607	583	487	473	615
BN5	758	713	690	581	568	662 ^b /692 ^c

^a (19% HF_{exc} at short-range and 65% HF_{exc} at long-range)

^b BN5 without alkyl unit; ^c BN5 with tert-butyl alkyl units

Table S3 Calculated the maximum absorption and emission energies and wavelengths

with B3LYP functional and different basis sets for the investigated experimental molecules.

Compd.	λ_{abs} (eV/nm)		Exp. (nm)	λ_{emi} (eV/nm)		Exp. (nm)
	6-31G(d)	def-TZVP		6-31G(d)	def-TZVP	
BN1	2.80/443	2.75/451	468	2.67/465	2.62/474	489
BN2	2.85/435	2.81/441	453	2.74/453	2.68/462	466
BN4	2.13/582	2.10/591	597	2.04/607	2.01/617	615
BN5	1.95/634	1.91/649	629 ^b /651 ^c	1.74/713	1.70/730	662 ^a /692 ^b

^a BN5 without alkyl unit; ^b BN5 with tert-butyl alkyl units

Table S4 Calculated bond lengths (indicated in Fig. 2 and Fig. S1) of the studied molecules at S_0 and S_1 states.

Compd.	S_0						S_1					
	l_1	l_2	l_3	l_4	l_5	l_6	l_1	l_2	l_3	l_4	l_5	l_6
BN1	1.54	1.40	1.40				1.55	1.40	1.40			
BN2	1.54	1.40	1.38	1.40	1.54		1.56	1.39	1.37	1.40	1.54	
BN3	1.54	1.36	1.36	1.36	1.54	1.54	1.58	1.37	1.37	1.37	1.55	1.55
BN4	1.55	1.39	1.40	1.55			1.53	1.40	1.40	1.53		
BN5	1.56	1.41	1.41	1.56	1.41	1.41	1.54	1.40	1.40	1.54	1.40	1.40

Table S5 Calculated the low-lying energies (E_{S_1}), the maximum absorption wavelengths (λ_{abs}), oscillator strengths (f), and transition compositions related to $S_0 \rightarrow S_1$ process for the investigated molecules in toluene.

Compd.	E_{S_1} (eV)	λ_{abs} (nm)	f	Transition configuration
BN1	2.80	443	0.5116	H \rightarrow L (0.99)

BN2	2.85	435	0.5060	H→L (0.95)
BN3	3.07	403	0.0000	H-1→L+1 (0.48); H→L+2 (0.48)
BN4	2.13	582	0.6441	H→L (0.99)
BN5	1.95	634	0.3878	H→L (0.99)

Table S6 Calculated oscillator strength and the square of the transition dipole moment (μ^2) for the investigated molecules relevant to absorption and emission processes.

Compd.	Abs.		Emi.	
	f	μ^2	f	μ^2
BN1	0.5116	7.4593	0.4395	6.7215
BN2	0.506	7.2525	0.2792	4.1677
BN3	0	0	0.006	0.0833
BN4	0.6441	12.3341	0.6028	12.04
BN5	0.3878	8.097	0.3392	7.9704

Table S7 Simulated FWHM at the maximum emission wavelength of the studied molecules.

Compd.	BN1	BN2	BN3	BN4	BN5
λ_{em} (nm)	465	453	422	607	713
FWHM _{Cal.} (nm/eV)	26/0.15	20/0.12	8/0.03	22/0.07	31/0.08
FWHM _{Exp.}	23/0.13	16/0.09	--	21/0.07	38/0.14